LMECA2640 MECHANICS OF COMPOSITE MATERIALS

PROJECT REPORT

Submitted by: Junaid AHMED

Negar MOHTADIFAR

Course: LMECA2640 Mechanics of Composite Materials

Submitted to: Prof. Issam DOGHRI

Date of submission: 10th June, 2022

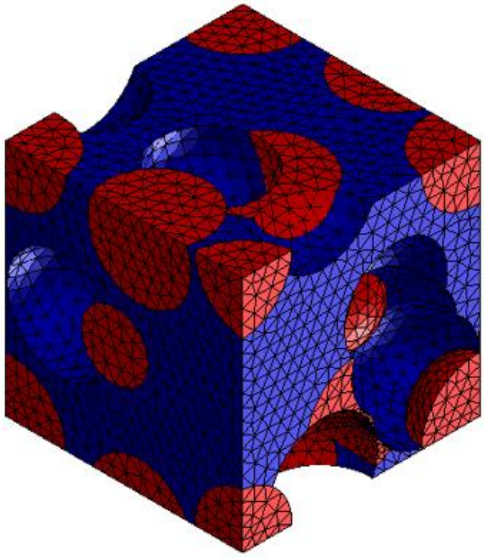

ÉCOLE POLYTECHNIQUE DE LOUVAIN

UNIVERSITÉ CATHOLIQUE DE LOUVAIN, BELGIUM

Table of Contents

Table of Figures

Table of Tables

1. Part I: Two-phase Materials, Spherical Inclusions

An RVE made of identical spherical inclusions which are randomly dispersed in the matrix phase is considered. Material properties corresponding to the matrix and the inclusions are listed in below table. It should be noted that the elastic modulus of the reinforcement phase is determined by the value of stiffness contrast ($E_{contrast} = \frac{E_1}{E_0}$).

Table 1 – Material properties of different constitutive phases of RVE

Phase	Young's Modulus (E_i) [Pa]	Poisson's Ratio (ν_i)	Density (ρ_i) [kg/m^3]
Matrix ($i = 0$)	3.42E+9	0.32	1100
Inclusion (Reinforcement) ($i = 1$)	$E_{contrast} \times E_0$	0.21	1.7

Next, two different mean-field models are used in order to homogenize the RVE: Mori-Tanaka (MT) and Differential Model (DM). These models are coded in MATLAB software to calculate effective bulk modulus ($\bar{\kappa}$) and effective shear modulus ($\bar{\mu}$) for different volume fractions of inclusions (v_1) as well as different stiffness contrasts:

$$v_1 = 10\%, 20\%, 30\%, 40\% \; and \; 50\%$$

$$\frac{E_1}{E_0} = 100, 50, 20, 10, 5 \; and \; 0 \; (which \; corresponds \; to \; cavities)$$

The results obtained from each model are reported in the next two sub-sections. It should be noted that all the codes are adjustable in such way that we can easily increase the number of inclusions' volume fraction to get smoother graphs.

1.1. Mori-Tanaka Mean-field Model (MT)

The values of homogenized shear and bulk moduli ($\bar{\mu}$ and $\bar{\kappa}$) for the RVE are calculated using MT relationships.

The normalized effective shear and bulk moduli ($\bar{\mu}_{norm} = \frac{\bar{\mu}}{\mu_0}$ and $\bar{\kappa}_{norm} = \frac{\bar{\kappa}}{\kappa_0}$) with respect to the shear and bulk moduli of the matrix phase (μ_0 and κ_0), are plotted for different volume fractions and stiffness contrasts in figures 1 and 2 by using this model. It should be noted that the zero volume fraction cases where $\bar{\mu} = \mu_0$ and $\bar{\kappa} = \kappa_0$ are also added to have better plots.

As we can see, by increasing the volume fraction of the inclusions in all cases except the cavity case ($\frac{E_1}{E_0} = 0$), both $\bar{\mu}$ and $\bar{\kappa}$ increase which is what we expected since the properties of the reinforcement phase are higher than of matrix phase, hence by increasing the volume fraction, we will enhance the RVE's mechanical properties. In the case of cavities, the properties of RVE degrade as it was expected; since the properties of the cavity are equal to zero.

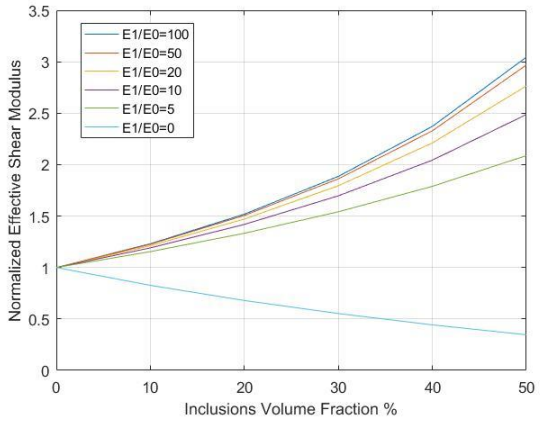

Figure 1 – Normalized effective shear modulus ($\frac{\bar{\mu}}{\mu_0}$) using MT model for different inclusions' volume fractions v_1 and stiffness contrasts $\frac{E_1}{E_0}$

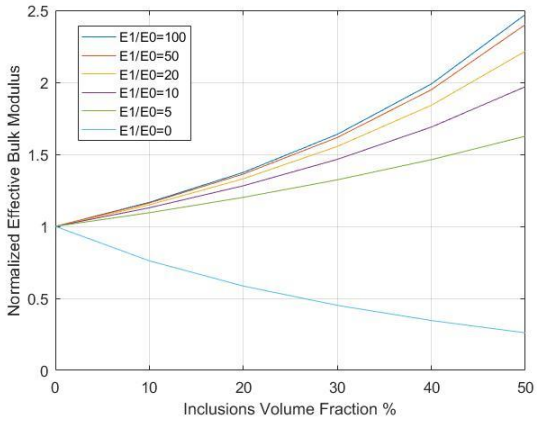

Figure 2 – Normalized effective bulk modulus ($\frac{\bar{\kappa}}{\kappa_0}$), using MT model for different inclusions' volume fractions v_1 and stiffness contrasts $\frac{E_1}{E_0}$

Moreover, we can clearly observe that by increasing the stiffness contrast (from zero to 100), the $\bar{\mu}$ and $\bar{\kappa}$ increase. Also, by comparing $\bar{\mu}_{norm}$ and $\bar{\kappa}_{norm}$ values in figures 1 and 2, we can see that the effect of changing $v_1$and $\frac{E_1}{E_0}$ is higher on $\bar{\mu}$ compared to $\bar{\kappa}$ (e.g., in the case of $v_1 = 50\%$ and $\frac{E_1}{E_0} = 100$, $\bar{\mu}_{norm} \approx 3$; however, $\bar{\kappa}_{norm} \approx 2.5$.)

1.2. Differential Mean-field Model (DM)

In DM method, inclusions are added progressively and step by step to reach the final expected volume fraction. In our code, we assumed to add the inclusion in N=300 steps. During each step, MT model is applied to compute the effective shear and bulk moduli of that step. The values of homogenized bulk and shear moduli for the RVE are calculated using MT relationships in each step. $\bar{\mu}_{norm}$ and $\bar{\kappa}_{norm}$, are plotted respectively for different volume fractions and stiffness contrasts in below figures.

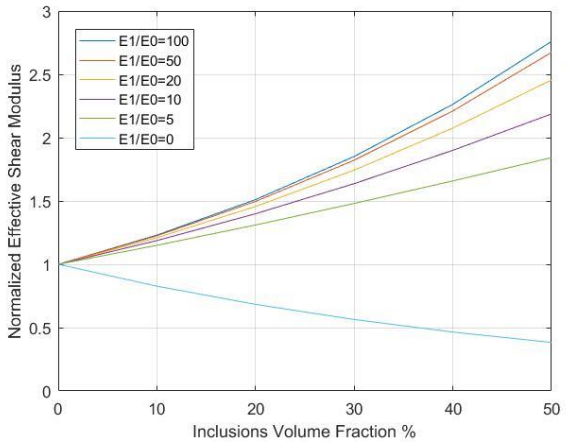

Figure 3 – Normalized effective shear modulus ($\frac{\bar{\mu}}{\mu_0}$), using DM for different inclusions' volume fractions v_1 and stiffness contrasts $\frac{E_1}{E_0}$

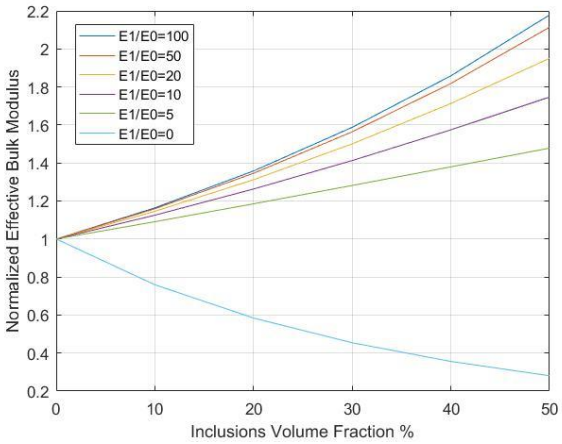

Figure 4 – Normalized effective bulk modulus ($\frac{\bar{\kappa}}{\kappa_0}$) using DM for different inclusions' volume fractions v_1 and stiffness contrasts $\frac{E_1}{E_0}$

As we can observe, similar trend of changes for $\bar{\mu}_{norm}$ and $\bar{\kappa}_{norm}$ is observed in both DM and MT models. This means that $\bar{\mu}$ and $\bar{\kappa}$ of the RVE are directly proportional to the stiffness contrast and volume fraction of inclusions (except the cavity case as explained in MT model in section 1.1).

In order to get a better understanding of the results of both mean-field models, in next section, we have compared them for three specific stiffness contrasts.

1.3. Comparison of the Two Mean-field Models (MT and DM)

In this section, we compare $\bar{\mu}_{norm}$ and $\bar{\kappa}_{norm}$ for 3 different stiffness contrasts ($\frac{E_1}{E_0} = 100, 20\ and\ 0$). The results are shown in below graphs.

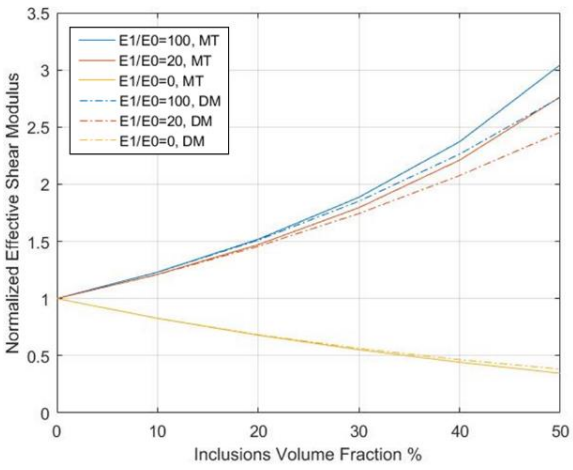

Figure 5 - Comparison of normalized effective shear modulus ($\frac{\bar{\mu}}{\mu_0}$), using MT and DM for different inclusions' volume fractions v_1 and 3 different stiffness contrasts ($\frac{E_1}{E_0} = 100, 20\ and\ 0$)

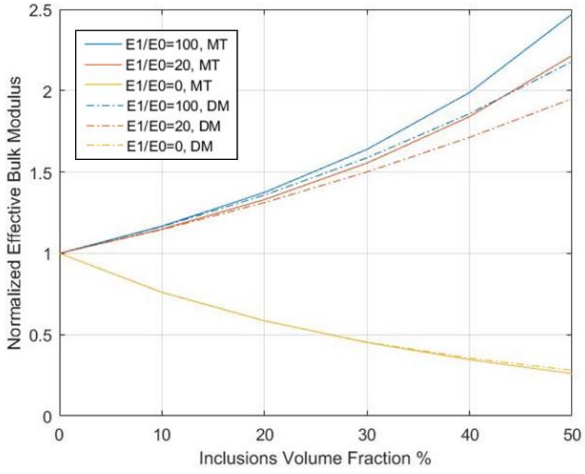

Figure 6 - Comparison of normalized effective shear modulus ($\frac{\bar{\kappa}}{\kappa_0}$), using MT and DM for different inclusions' volume fractions v_1 and 3 different stiffness contrasts ($\frac{E_1}{E_0} = 100, 20\ and\ 0$)

First, as we can see for the case of cavities ($\frac{E_1}{E_0} = 0$), the two models predict almost the same values for $\bar{\mu}$ and $\bar{\kappa}$. However, by increasing the volume fraction of cavities, they diverge slightly.

Moreover, we observe that the predicted properties using the two mean-field models are closer in smaller volume fractions. However, as we increase the volume fractions, they start to diverge at around $v_1 = 20\%$. (This divergence is more intense for cases of $\frac{E_1}{E_0} \neq 0$ compared to the cavity case).

Furthermore, we can see that the predicted $\bar{\mu}$ and $\bar{\kappa}$ by MT method are higher than the ones calculated using the DM.

2. PART II: Three-phase Materials, Spherical Inclusions

An RVE made of two types of spherical inclusions embedded in the matrix phase is considered. The first inclusion ($i = 1$) is considered to be the solid one and its mechanical properties are same as the one listed in table 1. The second inclusion is considered to be cavity ($i = 2$). Matrix phase properties are identical to the ones in table 1. It should be noted that the elastic modulus of the reinforcement phase (inclusions 1) is determined by the value of stiffness contrast ($\frac{E_1}{E_0}$).

Four different homogenization methods are used in order to obtain the RVE properties:

1. 2-step method
2. 2-level method-first variant
3. 2-level method-second variant
4. Differential Model (DM).

These models are coded in MATLAB software to calculate effective bulk modulus ($\bar{\kappa}$) and effective shear modulus ($\bar{\mu}$) for different inclusions' volume fractions ($v_1 and\ v_2$) of inclusions as well as different stiffness contrasts:

$$v_1 = v_2 = 5\%, 10\%, 15\%, 20\%\ and\ 25\%$$

$$\frac{E_1}{E_0} = 100, 50, 20, 10\ and$$

The results obtained from each model are reported in the next four sub-sections.

2.1. Two-step Method

In this method the matrix phase is split in half, and each of the inclusion phases (solid and cavity) are homogenized with one half of the matrix phase using MT model. After computing the properties of each part, they are homogenized together using Voigt method.

$\bar{\mu}_{norm}$ and $\bar{\kappa}_{norm}$, are plotted in the figures 7 and 8 for different volume fractions ($v_1 + v_2 = 2v_1$) and different stiffness contrasts.

We can observe that by increasing the volume fractions, $\bar{\mu}$ increases, however, $\bar{\kappa}_{norm}$ first decreases and after a specific volume fraction, it starts to increase. This specific volume fraction changes based on the stiffness contrast of the solid inclusions. In lower stiffness contrasts, it happens in higher volume fractions meaning that since the solid inclusions are not that stiff compared to the matrix phase, the effect of cavities in decreasing the overall RVE properties is higher.

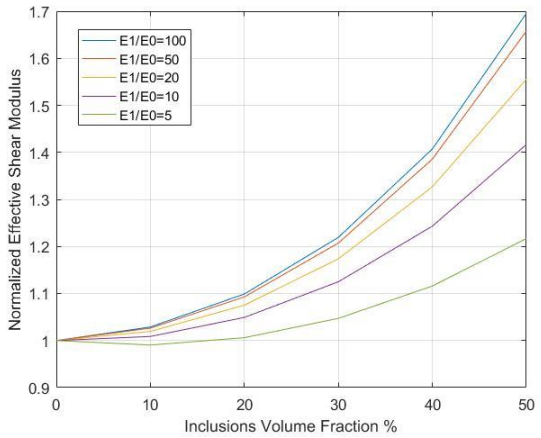

Figure 7 – Normalized effective shear modulus ($\frac{\bar{\mu}}{\mu_0}$), using two-step method for different inclusions' volume fractions $v_1 + v_2$ and stiffness contrasts $\frac{E_1}{E_0}$

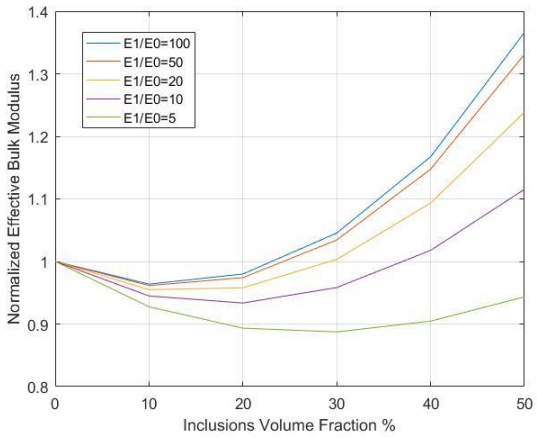

Figure 8 – Normalized effective bulk modulus ($\frac{\bar{\kappa}}{\kappa_0}$), using two-step method for different inclusions' volume fractions $v_1 + v_2$ and stiffness contrasts $\frac{E_1}{E_0}$

2.2. Two-level Method, First Variant

In this method first inclusions 1 (solid) are added to the matrix and homogenized. The volume fraction in lower level is calculated based on the equation provided in the provided reference paper. Next, inclusions 2 (cavities) are embedded in a new matrix which its properties are taken from the deep level's homogenized results. In both level MT is applied. It should be noted that the Poisson's ratio as well as the shear and bulk parts of Eshelby's tensor are recomputed and updated based on the homogenized properties after the deep level.

$\bar{\mu}_{norm}$ and $\bar{\kappa}_{norm}$, are plotted for different volume fractions ($v_1 + v_2 = 2v_1$) and stiffness contrasts of the solid inclusions in below figures by using this model:

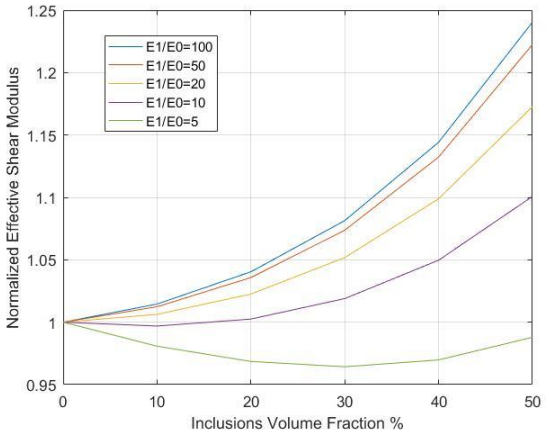

Figure 9 – Normalized effective shear modulus ($\frac{\bar{\mu}}{\mu_0}$), using two-level method, first variant for different inclusions' volume fractions $v_1 + v_2$ and stiffness contrasts $\frac{E_1}{E_0}$

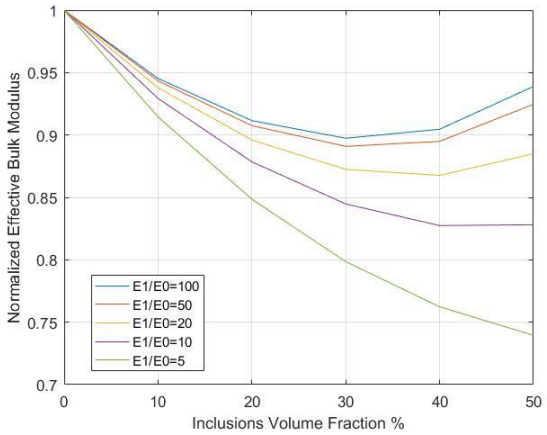

Figure 10 – Normalized effective bulk modulus ($\frac{\bar{\kappa}}{\kappa_0}$), using two-level method, first variant for different inclusions' volume fractions $v_1 + v_2$ and stiffness contrasts $\frac{E_1}{E_0}$

We can see that except the case where the stiffness contrast is equal to 5, $\bar{\mu}_{norm}$ of the homogenized RVE increases as the volume fraction increases, and we have higher $\bar{\mu}$ values compared to that of the matrix phase. This means that the positive effect of solid inclusions on the $\bar{\mu}$ is larger than the degrative effect of cavities. In the case of stiffness contrast equal to 5, first we have a decrease in the normalized effective shear modulus then after a specific volume, it starts to increase.

In all cases of volume fractions and stiffness contrasts, $\bar{\kappa}$ is lower than that of the matrix. It means that the negative effect of cavities on $\bar{\kappa}$ is larger than to be compensated by the solid inclusions. However, in higher stiffness contrasts after a specific value of volume fraction, the descending trend of $\bar{\kappa}_{norm}$ stops and it starts to increase, but still not enough to completely cancel the negative effect of cavities on $\bar{\kappa}$.

2.3. Two-level Method, Second Variant

This method is quite similar to the previous one. The only difference is that in the deep level, we add the cavities, and then after homogenizing using MT method, the solid inclusions are embedded in the homogenized RVE of first level. $\bar{\mu}_{norm}$ and $\bar{\kappa}_{norm}$, are plotted in the figures below for different volume fractions ($v_1 + v_2 = 2v_1$) and different stiffness contrasts.

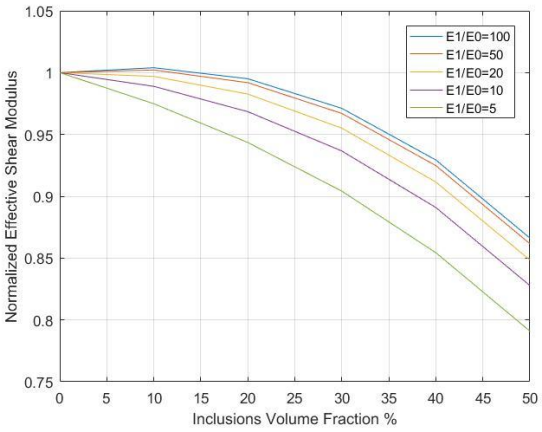

Figure 11 – Normalized effective shear modulus ($\frac{\bar{\mu}}{\mu_0}$), using two-level method, second variant for different inclusions' volume fractions $v_1 + v_2$ and stiffness contrasts $\frac{E_1}{E_0}$

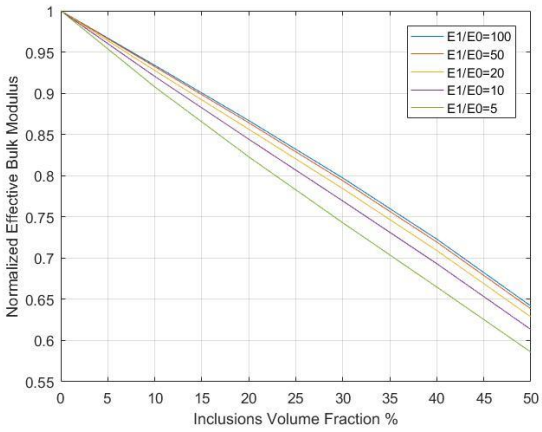

Figure 12 – Normalized effective bulk modulus ($\frac{\bar{\kappa}}{\kappa_0}$), using two-level method, second variant for different inclusions' volume fractions $v_1 + v_2$ and stiffness contrasts $\frac{E_1}{E_0}$

As we can observe, both $\bar{\mu}$ and $\bar{\kappa}$ decrease as we increase the volume fraction. This means that in all possible cases, the effective properties ($\bar{\mu}$ and $\bar{\kappa}$) have degraded compared to the initial matrix properties and we can conclude that the negative effect of cavities in decreasing the properties is much higher than the positive effect of solid inclusions. Also, we observe that the slope of decrement of the properties is almost constant for $\bar{\kappa}_{norm}$, but as we increase the volume fraction, the descending slope of $\bar{\mu}_{norm}$ gets steeper meaning the negative effect of cavities becomes greater in higher volume fraction.

2.4. Differential Method (DM)

This method is similar to the method explained in subsection 1.2 where we used DM for two-phase materials. The difference is in the progressive increment of small volume fractions; in odd steps, we add the solid inclusions and homogenize using MT, and in the even ones, we add the cavities and homogenize. It should be noted that the bulk and shear parts of Eshelby's tensor are updated before adding inclusions in each step based on the homogenized properties obtained in the previous step.

$\bar{\mu}_{norm}$ and $\bar{\kappa}_{norm}$ are plotted for different volume fractions ($v_1 + v_2 = 2v_1$) and stiffness contrasts in below figures.

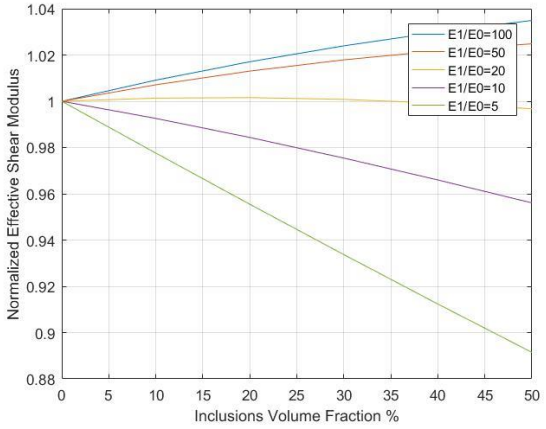

Figure 13 – Normalized effective shear modulus ($\frac{\bar{\mu}}{\mu_0}$), using DM for different inclusions' volume fractions $v_1 + v_2$ and stiffness contrasts $\frac{E_1}{E_0}$

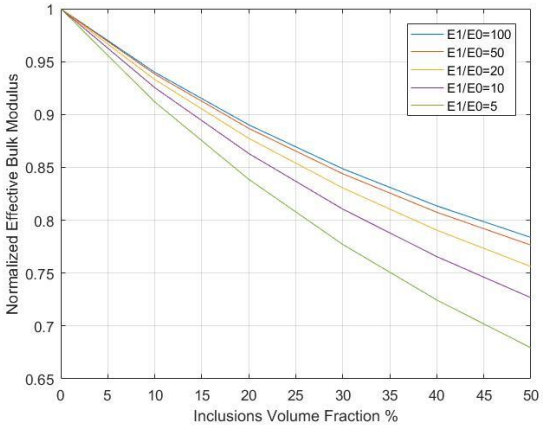

Figure 14 – Normalized effective bulk modulus ($\frac{\bar{\kappa}}{\kappa_0}$), using DM for different inclusions' volume fractions $v_1 + v_2$ and stiffness contrasts $\frac{E_1}{E_0}$

$\bar{\mu}_{norm}$ increases in cases with higher stiffness contrast by increasing the volume fraction. But we observe decrease of $\bar{\kappa}_{norm}$ in lower values of stiffness contrasts.

$\bar{\kappa}$ decreases regardless of the volume fraction and stiffness contrast meaning the effect of cavities on degrading $\bar{\kappa}$ is much higher than the positive effect of solid inclusions. After homogenizing via DM method, we will end up with lower bulk moduli compared to the matrix bulk modulus.

2.5. Comparison of the Four Models

In this section, we compare $\bar{\mu}_{norm}$ and $\bar{\kappa}_{norm}$ obtained using 4 different methods for the case of stiffness contrasts equal to 50 and different volume fractions. The results are shown in below graphs.

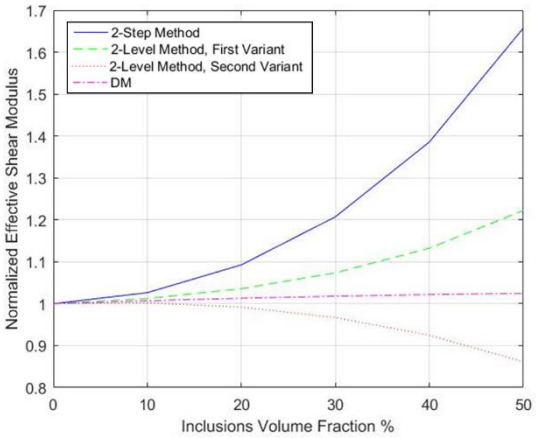

Figure 15 – Comparison of normalized effective shear modulus ($\frac{\bar{\mu}}{\mu_0}$), using four proposed methods for different inclusions' volume fractions $v_1 + v_2$ and a specific stiffness contrasts ($\frac{E_1}{E_0} = 50$)

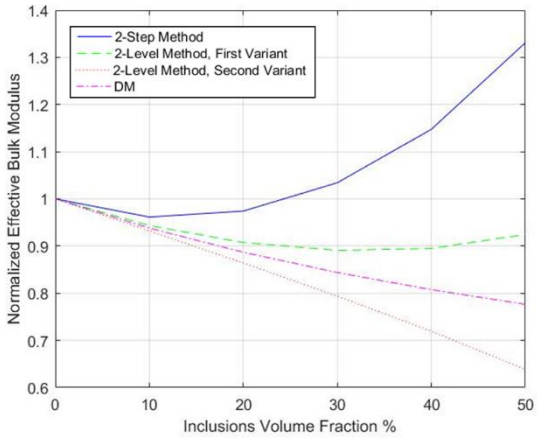

Figure 16 – Comparison of normalized effective shear modulus ($\frac{\bar{\kappa}}{\kappa_0}$), using four proposed methods for different inclusions' volume fractions $v_1 + v_2$ and a specific stiffness contrasts ($\frac{E_1}{E_0} = 50$)

As we observe in the above figures, the predicted properties using each method is completely different from the other methods. However, the predicted results obtained from all four methods in smaller volume fractions are closer to each other but as we increase the volume fractions, they deviate from each other.

In order to see which homogenization method predicts the effective properties of the composite better, we need to do experimental test or high precision FE simulation and compare it with the results obtained from each of these homogenization methods.

3. PART III: Two and Three-phase Materials, Non-spherical Inclusions; Using Digimat-MF

3.1. Digimat Homogenization Using Mean Field Scheme

Following steps were performed to setup the homogenization setup in Digimat-MF software.

- The materials were defined with the properties listed in table 1.
- Phases were created for the RVE. These can be matrix and inclusion phase with their corresponding material. When the stiffness contrast is zero, the inclusions act as cavities and a new phase was created using void properties. For all phases, a respective volume fraction is assigned.
- In case of all 3 phases (matrix, inclusions and cavities), multi-level method is defined for the homogenization.
- The homogenization scheme is set to be Mori-Tanaka.
- The aspect ratios are varied. As we increase the aspect ratio, the inclusion changes from platelet to spherical to fiber shape. Following figures show the inclusions with different aspect ratios.

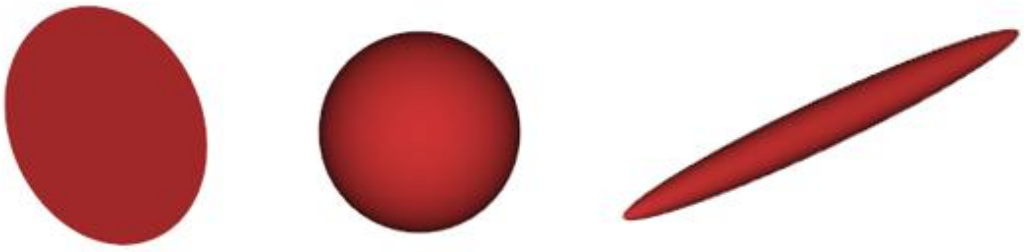

Figure 17 – Inclusion with aspect ratio equal to 0.001 (left), 1 (center), and 10 (right)

- The orientation of inclusions is set to be along the axis 1 as shown in the following figure.

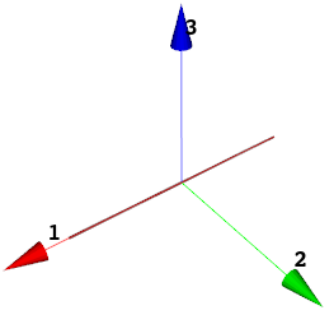

Figure 18 – Orientation of inclusions

- A uniaxial strain as a monotonic load is applied on the microstructures along the direction 1 as shown in the following figure.

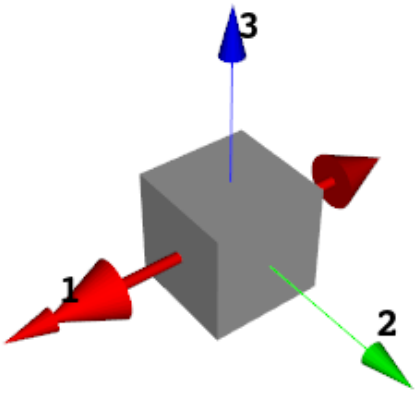

Figure 19 – Uniaxial strain along direction 1

- From Digimat-MF, effective properties are obtained. The effective elastic modulus of the RVE is given by E_{22}, effective shear modulus as μ_{23} and effective Poisson's ratio as υ_{23}.

3.2. Two-phase RVE

We first consider a two phase RVE with non-spherical aligned inclusions. The volume fraction of inclusion v_1 for this study is set to be 30%. We vary the aspect ratio of the inclusions and the stiffness contrast of the RVE as follows.

- Aspect ratio of the inclusions: 100, 50, 20, 10, 5, 0.5, 0.2, 0.1, and 0.001
- Stiffness contrast $\frac{E_1}{E_0}$: 100, 50, 20, 10, 5, and 0

Note that when the stiffness contrast is equal to zero, the inclusions correspond to the cavities with zero stiffness. We vary the aspect ratio for each value of stiffness contrast. We obtain 6 different curves for 6 different stiffness contrasts and we observe the variation of the normalized effective engineering properties with the aspect ratios.

For the normalized effective engineering properties, we consider the $\bar{\mu}$ and $\bar{\kappa}$ of the RVE normalized by the respective matrix properties as below.

$$\mu = \frac{E}{2(1+\upsilon)} \quad ; \quad Normalized\ effective\ \mu = \bar{\mu}_{norm} = \frac{\mu_{23}}{\mu_0}$$

$$K = \frac{E}{3(1-2\upsilon)} \quad ; \quad Normalized\ effective\ \kappa = \bar{\kappa}_{norm} = \frac{K_{23}}{K_0} = \frac{1}{K_0}\frac{E_{22}}{3(1-2\upsilon_{23})}$$

where, κ = Bulk Modulus $\left(\frac{N}{m^2}\right)$ and μ = Shear Modulus $\left(\frac{N}{m^2}\right)$. The index 0 refers to the matrix.

The variations of $\bar{\mu}_{norm}$ with the aspect ratio of inclusions for different stiffness contrasts are plotted as below.

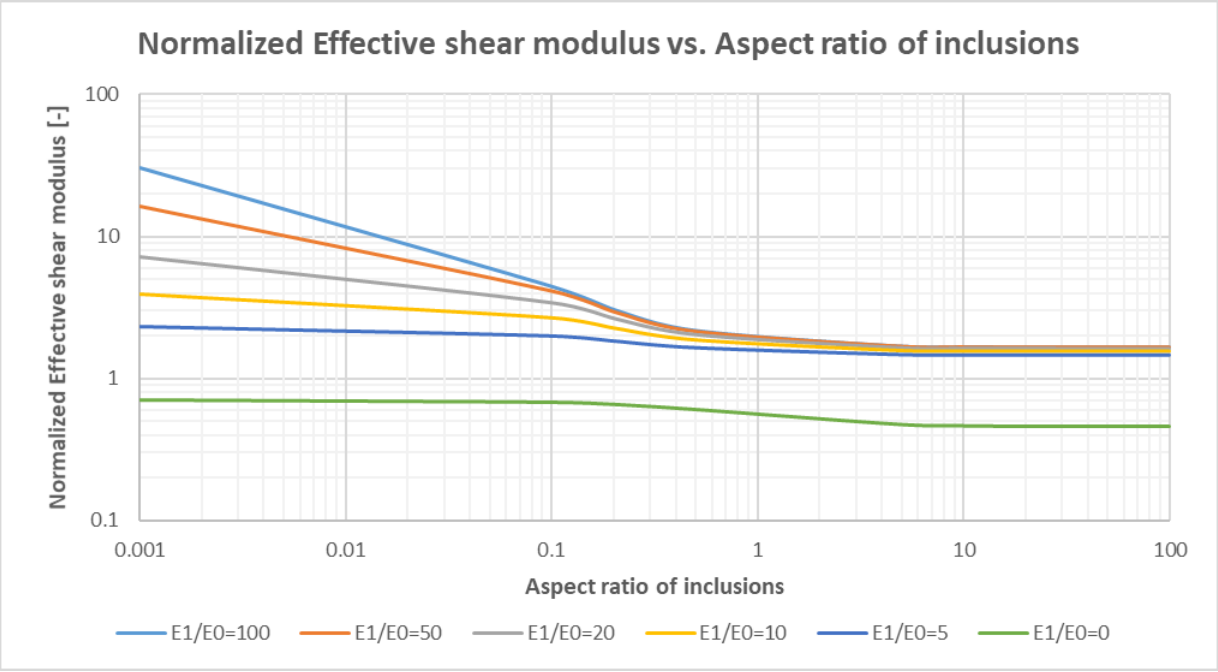

Figure 20 – $\bar{\mu}_{norm}$ vs aspect ratio of inclusions

From the above plot, we can observe that

- The normalized effective shear moduli $\bar{\mu}_{norm}$ are the highest for the highest stiffness contrast.
- For all non-zero stiffness contrasts, $\bar{\mu}_{norm}$ is greater than 1. This indicates that presence of inclusions with non-zero stiffness contrast always contribute towards increasing the $\bar{\mu}$ of the RVE than that of matrix for any aspect ratio.
- As the stiffness contrast decreases from 100 to 0, both $\bar{\mu}_{norm}$ and the change of $\bar{\mu}_{norm}$ with respect to aspect ratios of the inclusions decrease as the curves change from steeper to flatter. This means that stiffness contrast in the RVE significantly effects $\bar{\mu}$.
- As the aspect ratios of the inclusions change from 0.001 to 0.5 i.e. as the inclusions change from platelets to near-spherical, $\bar{\mu}_{norm}$ decreases. The critical value for aspect ratio is ~0.5 for this change.
- From aspect ratios 0.5 to 100, $\bar{\mu}_{norm}$ remains approximately constant. Thus, the change in the shape of inclusions from ellipsoidal to fiber does not affect the shear modulus significantly.
- For all non-zero stiffness contrasts, $\bar{\mu}_{norm}$ converges to approximately similar values.
- For stiffness contrast equal to zero (cavities instead of solid inclusions), $\bar{\mu}_{norm}$ converges to a value which is below 1 and much lower than the values for other stiffness contrasts. When there are only cavities present, the shear modulus of the RVE is always lower than that of the matrix.

The variations of $\bar{\kappa}_{norm}$ with the aspect ratio of inclusions for different stiffness contrasts are plotted as below.

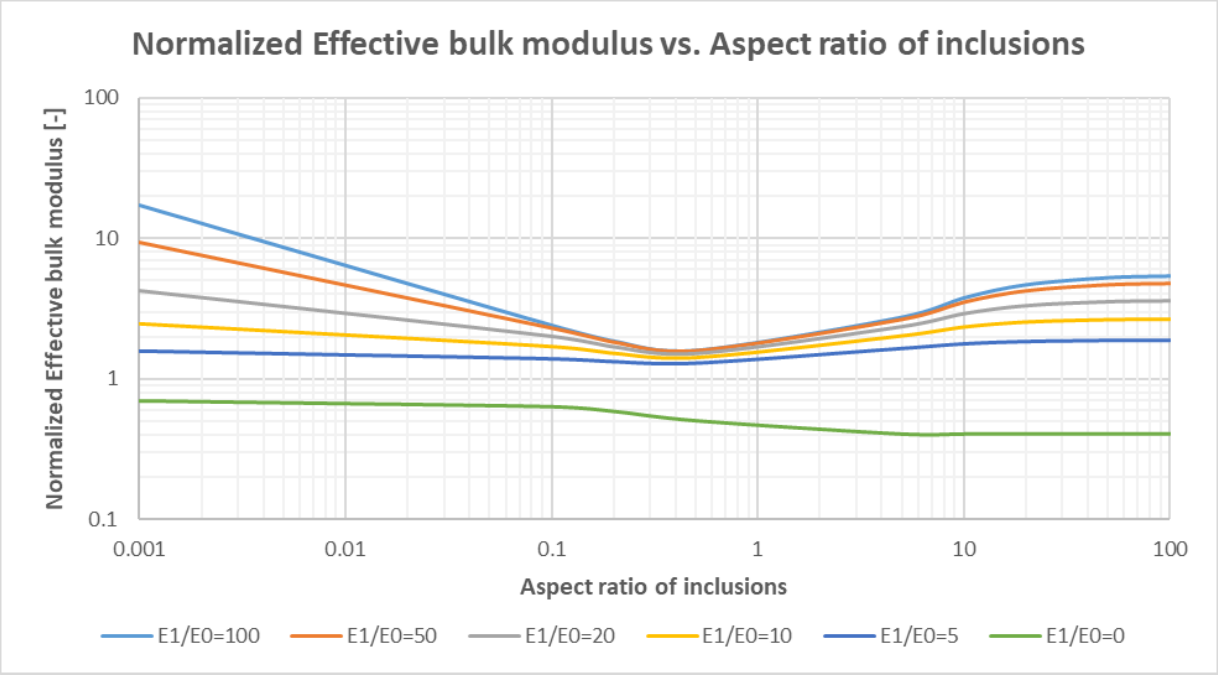

Figure 21 – $\bar{\kappa}_{norm}$ vs aspect ratio of inclusions

From the above plot, we can observe that,

- $\bar{\kappa}_{norm}$ are the highest for the highest stiffness contrast.
- Since all $\bar{\kappa}_{norm}$ are greater than 1 for non-zero stiffness contrasts, so we can conclude that adding the inclusions increases $\bar{\kappa}$ of the RVE, irrespective of the aspect ratios.
- For the non-zero stiffness contrasts, as the aspect ratios of the inclusions change from 0.001 to 0.5, $\bar{\kappa}_{norm}$ decreases and approach a critical value. This indicates that changing the shape of the inclusions from platelets to near spherical results in decrease of the ability of the RVE to resist compression.
- For the non-zero stiffness contrasts, from aspect ratios 0.5 to 100, $\bar{\kappa}_{norm}$ first increases and then reaches an approximately constant value. Thus, the ability of RVE to resist compression increases.
- For the stiffness contrast equal to zero (cavities), $\bar{\kappa}_{norm}$ first remains almost constant from aspect ratio equal to 0.001 to 0.1, then it decreases till aspect ratio equal to 10 and then it becomes constant. In all cases, it remains below 1 which means that adding cavities decrease the ability of the RVE to resist compression.

3.3. Three-phase RVE

Now we consider a three phase RVE which has non-spherical aligned inclusions. The solid inclusions (index 1) are prolate spheroids, and the cavities (index 2) are platelets (oblate spheroids). All inclusions have the same volume fraction ($v_1 = v_2 = 25\%$).

We use the two-level method in Digimat-MF in which one phase is inclusion and the other is cavity (void) along with the matrix phase. We have two cases:

3.3.1. Case 1: Spherical Solid Inclusions and Oblate Cavities

In this case, the aspect ratio of solid inclusions is kept to be 1 i.e. they are spherical. We vary the aspect ratio of the cavities and the stiffness contrast of the RVE as below.

- Aspect ratio of the cavities: 1, 0.5, 0.2, 0.1, and 0.001
- Stiffness contrast $\frac{E_1}{E_0}$: 100, 50, 25, 10, 5, and 0

The variations of $\bar{\mu}_{norm}$ and $\bar{\kappa}_{norm}$ with the aspect ratio of cavities are shown in the plots below.

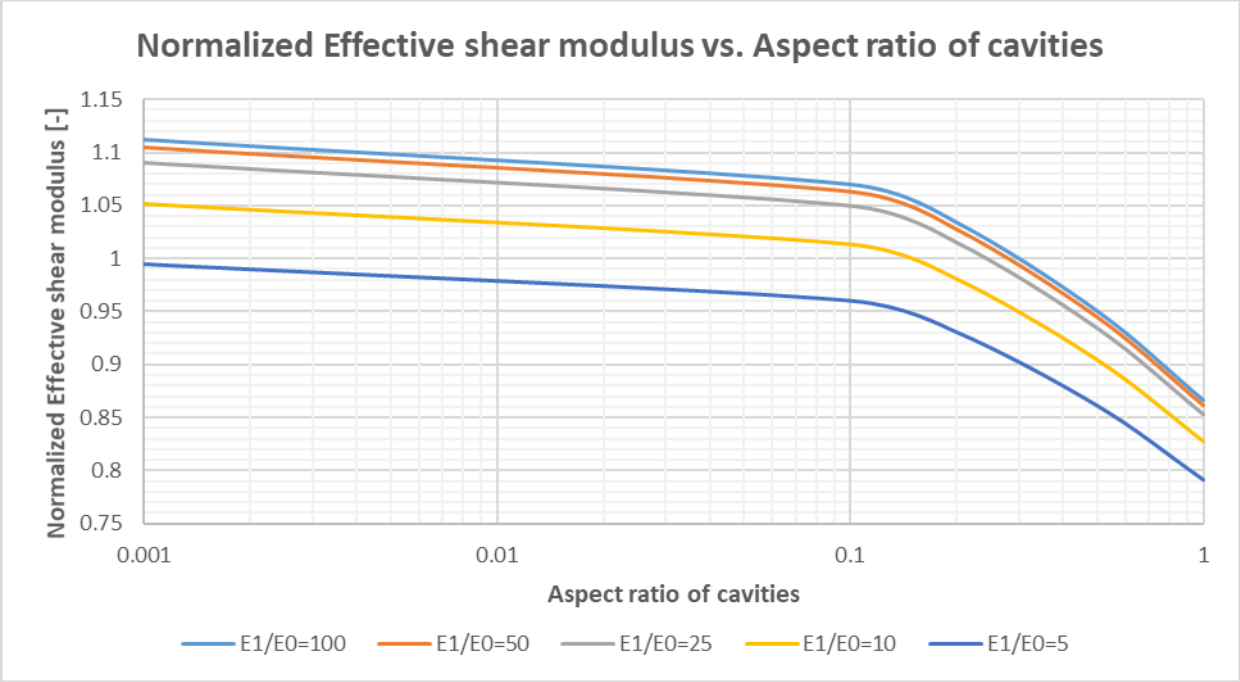

Figure 22 – $\bar{\mu}_{norm}$ vs aspect ratio of cavities

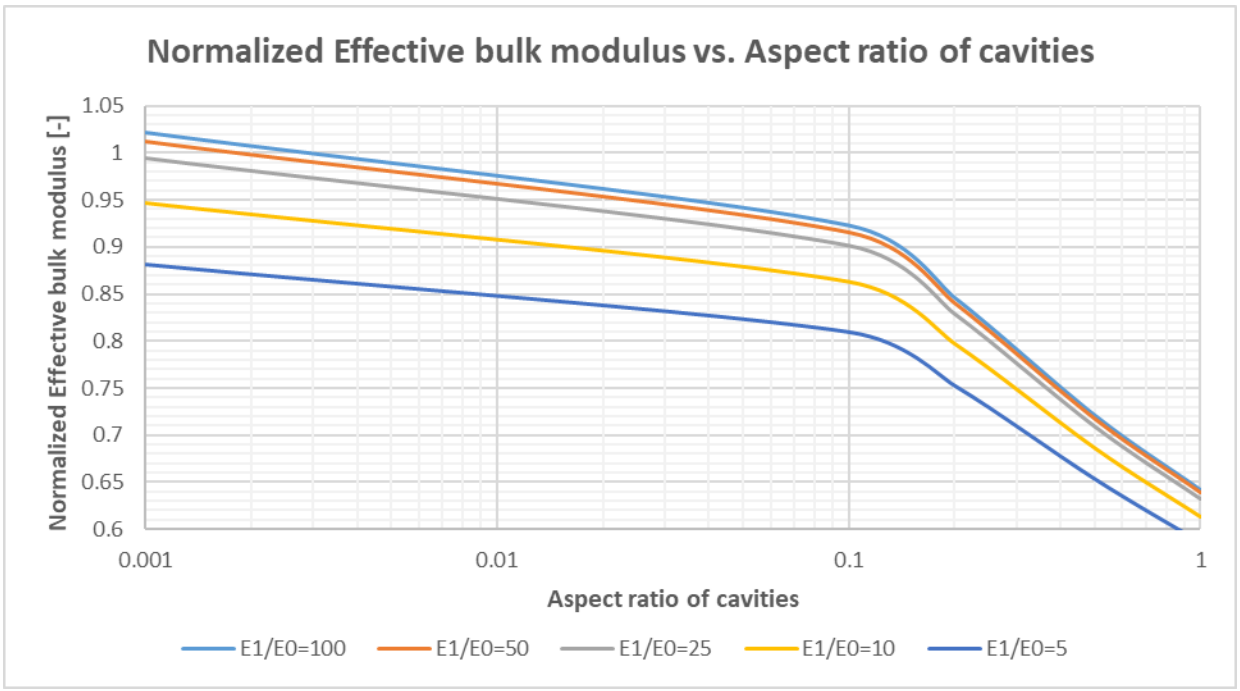

Figure 23 – $\bar{\kappa}_{norm}$ vs aspect ratio of cavities

As it can be observed from the above plots,

- $\bar{\mu}_{norm}$ and $\bar{\kappa}_{norm}$ are the highest for the highest stiffness contrast i.e. 100.
- $\bar{\mu}_{norm}$ and $\bar{\kappa}_{norm}$ decrease with the decrease in the stiffness contrast of the RVE.
- $\bar{\mu}_{norm}$ and $\bar{\kappa}_{norm}$ decrease with the increase in the aspect ratio of the oblate cavities.

- The slopes of the $\bar{\mu}_{norm}$ and $\bar{\kappa}_{norm}$ curves become steeper after aspect ratio increases between 0.1 to 1. This means that $\bar{\mu}_{norm}$ and $\bar{\kappa}_{norm}$ change significantly after 0.1. Thus cavities aspect ratio 0.1 is the critical value.
- Since both $\bar{\mu}_{norm}$ and $\bar{\kappa}_{norm}$ reach a value less than 1 with spherical cavities, it indicates that the spherical cavities in the RVE results in the decrease of shear and bulk modulus of the matrix.

3.3.2. Case 2: Spherical Cavities and Prolate Reinforcements

In this case, the aspect ratio of cavities is kept to be 1 i.e. they are spherical. We vary the aspect ratio of the prolate reinforcements and the stiffness contrast of the RVE as below.

- Aspect ratio of the reinforcements: 1, 10, 20, 50, and 100
- Stiffness contrast $\frac{E_1}{E_0}$: 100, 50, 25, 10, 5, and 0

The variations of $\bar{\mu}_{norm}$ with the aspect ratio of the reinforcements is shown in the plot below.

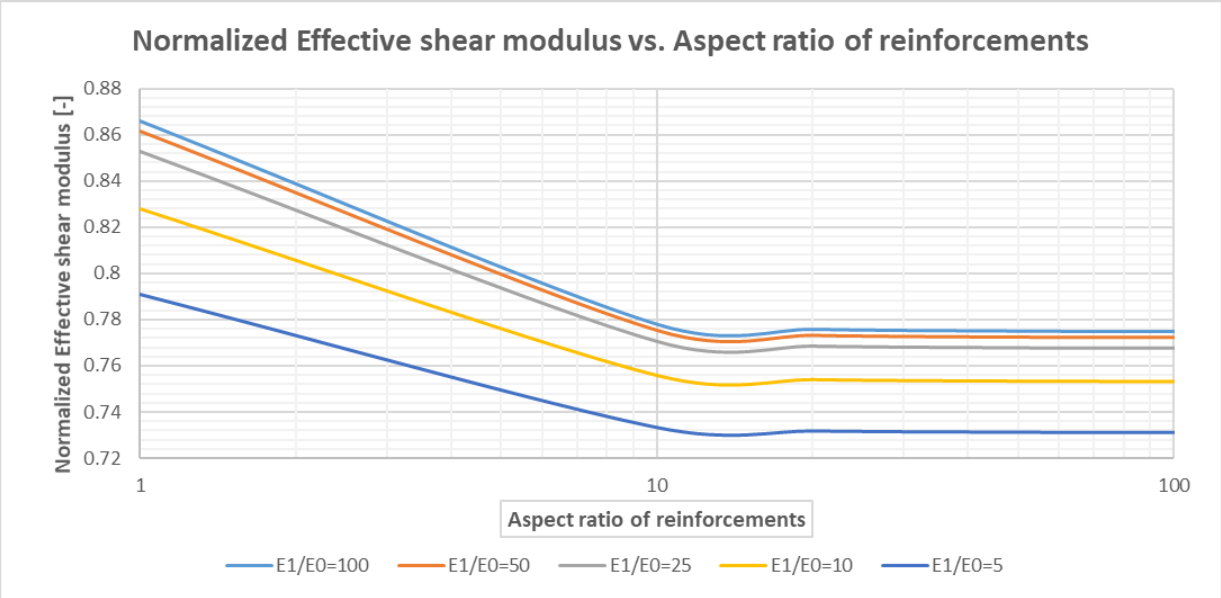

Figure 24 – $\bar{\mu}_{norm}$ vs aspect ratio of reinforcements

As it can be observed from the above plot,

- All values of $\bar{\mu}_{norm}$ are less than 1. This corroborates with our findings from the previous subsection in which $\bar{\mu}_{norm}$ was less than 1 for spherical cavities irrespective of the contrast ratio.
- $\bar{\mu}_{norm}$ are the highest for the highest stiffness contrast i.e. 100.
- $\bar{\mu}_{norm}$ decreases with the decrease in the stiffness contrast of the RVE.
- $\bar{\mu}_{norm}$ decreases as we increase the aspect ratio from 1 to 10. Further increase in aspect ratio between 10 to 100 results in the $\bar{\mu}_{norm}$ approaching a constant value while varying the aspect ratios. This means that the aspect ratio 10 of the reinforcements is critical after which there is no significant change in $\bar{\mu}_{norm}$.

The variations of $\bar{\kappa}_{norm}$ with the aspect ratio of the reinforcements is shown in the plot below.

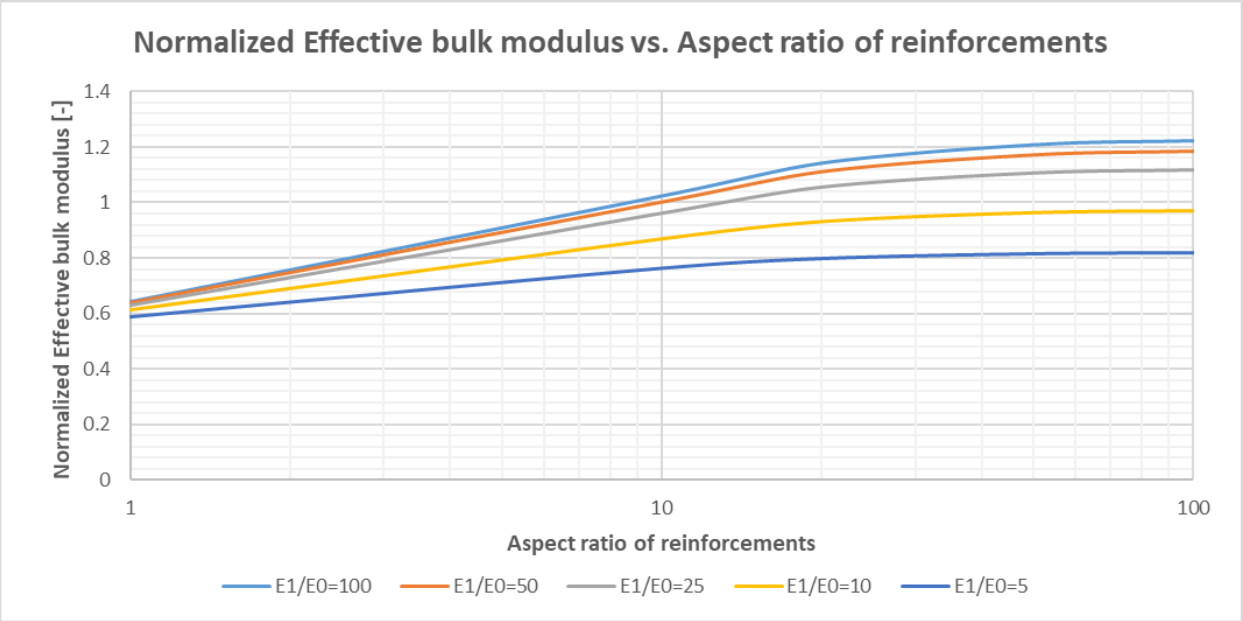

Figure 25 – $\bar{\kappa}_{norm}$ vs aspect ratio of reinforcements

As it can be observed from the above plot,

- For stiffness contrast less than and equal to 10, $\bar{\kappa}_{norm}$ is always less than 1. This results in the decrease of matrix ability to resist compression for all aspect ratios for the mentioned stiffness contrast range. Beyond this range, $\bar{\kappa}_{norm}$ increases indicating the increase in the bulk modulus of the RVE.
- $\bar{\kappa}_{norm}$ are the highest for the highest stiffness contrast i.e. 100.
- $\bar{\kappa}_{norm}$ decreases with the decrease in the stiffness contrast of the RVE.
- $\bar{\kappa}_{norm}$ increases significantly as we increase the aspect ratio from 1 to 30. Further increase in aspect ratio between 30 to 100 results in the very slight change in $\bar{\kappa}_{norm}$. Thus as we approach fiber inclusions, $\bar{\kappa}_{norm}$ achieves a constant value.
- The change in $\bar{\kappa}_{norm}$ with the aspect ratio of the reinforcement increases as we increase the stiffness contrast from 5 to 100.

4. PART IV: Two and Three-phase Materials; Using Digimat-FE

4.1. Digimat Homogenization Using Finite Element Analysis

The materials and phases are kept the same as that in the Digimat Mean Field Homogenization. The material properties and phase volume fractions are varied according to the prescribed values. The number of inclusions are specified and the mesh is generated. The orientation of inclusions is specified to be perpendicular to the 3rd axis. Mesh quality is checked by comparing the volume fraction of generated inclusions in the RVE mesh to that of the prescribed respective volume fraction of the inclusion. The two volume fractions need to be approximately close to each other for a good quality mesh. The number of inclusions are varied to achieve the optimal mesh quality and volume fractions. The number of mesh elements was kept below 100,000 to reduce the computational time.

In some cases, the interpenetration of inclusions or the size reduction or both were allowed to optimize the placement of the inclusions in the RVE for a good quality mesh. For each aspect ratio, the number of inclusions and the RVE size is changed to obtain the optimal mesh.

Following figures show the two RVEs and their mesh.

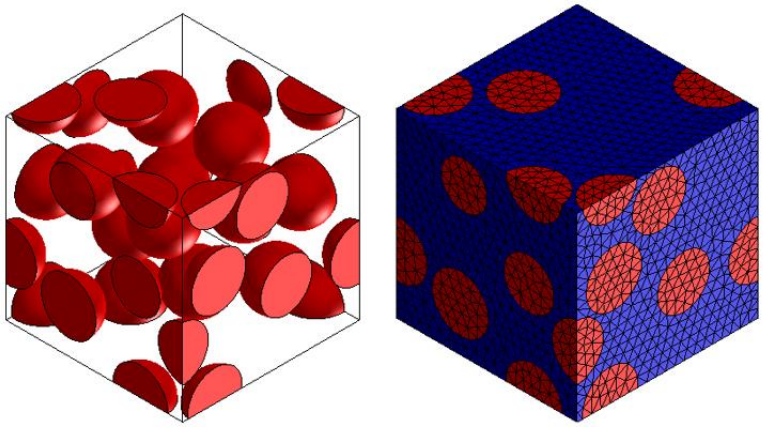

Figure 26 - RVE showing reinforcements (left) and meshed RVE (right)

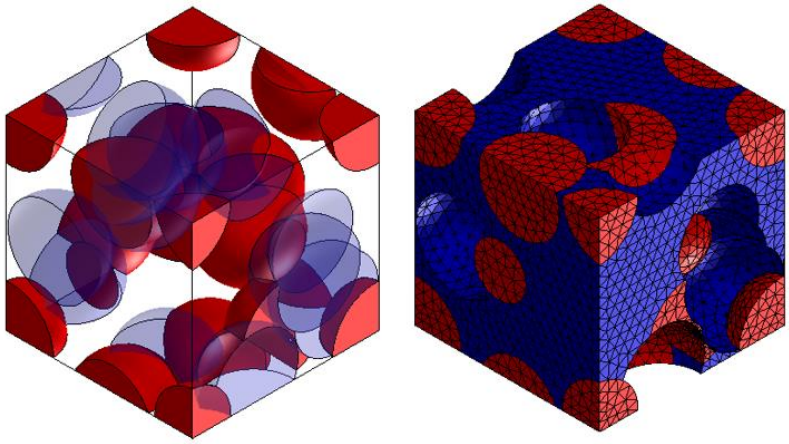

Figure 27 - RVE showing reinforcements and voids (left) and meshed RVE (right)

E_{22}, μ_{23} and ν_{23} are obtained for each analysis and normalized with the respective properties of the matrix.

We consider one stiffness contrast for the RVE i.e. $\frac{E_1}{E_0} = 100$. Four types of microstructures are considered which are listed below.

1. Two-phase with spherical reinforcements
2. Two-phase with prolate reinforcements
3. Three-phase with spherical cavities and prolate reinforcements
4. Three-phase with spherical reinforcements and oblate cavities

Analyses are performed on Digimat-FE on these microstructures and comparative studies are performed as explained in the next sections.

4.2. Two-phase with Spherical Reinforcements

A comparative study is performed between the results obtained from the code using Mori-Tanaka scheme in subsection 1.1 and those from Digimat-FE. The plot showing the comparative values is given as below.

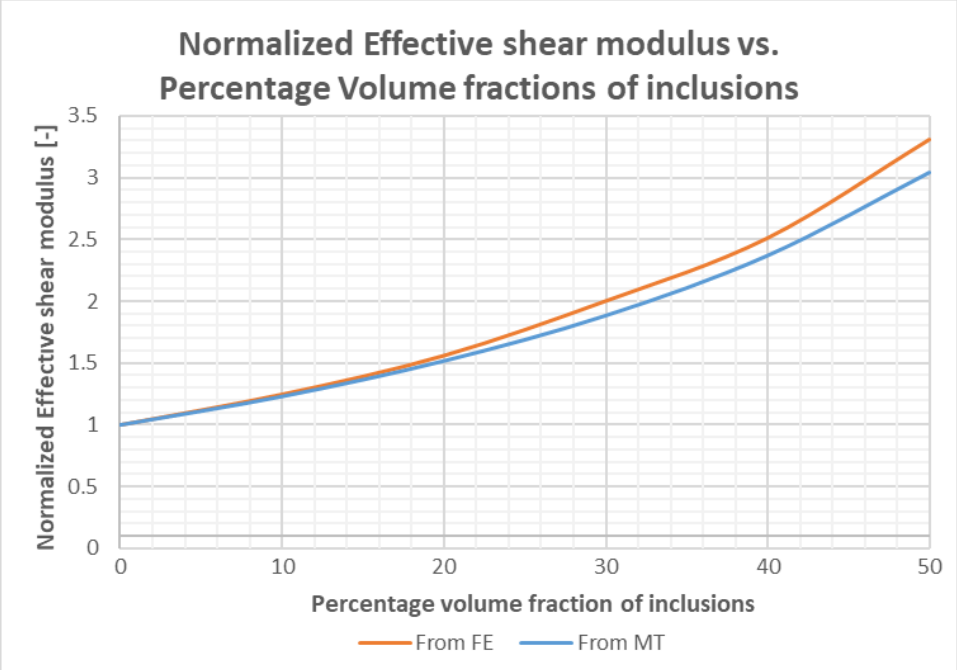

Figure 28 – $\bar{\mu}_{norm}$ vs percent volume fractions of inclusions

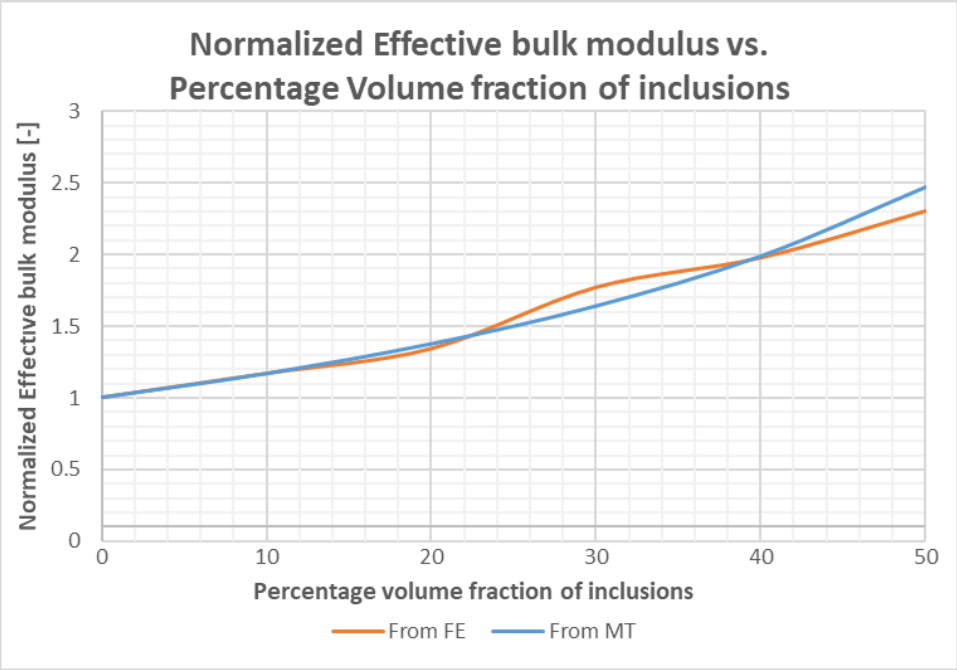

Figure 29 – $\bar{\kappa}_{norm}$ vs percent volume fractions of inclusions

We observe that as we increase the volume fraction of the inclusions, the error between the normalized effective shear and bulk moduli increases. This is because, the increase of volume fraction of the inclusions should be accompanied with the increase in the number of inclusions for uniform distribution of inclusions inside the RVE. This decreases the size of the inclusions and thus the mesh details become complicated. This results in very high number of mesh elements and thus a great computational time. To avoid this, we compromise a little on mesh quality which results in the error for high volume fractions.

4.3. Two-phase with Prolate Reinforcements

The results obtained from Digimat-MF for the two-phase microstructure with prolate reinforcement calculated in subsection 3.2 are compared with the results obtained from Digimat-FE. The aspect ratio of the reinforcements is varied between 0.001 to 100.

The variations of $\bar{\mu}_{norm}$ and $\bar{\kappa}_{norm}$ with the aspect ratio of the reinforcements are shown in the plots below.

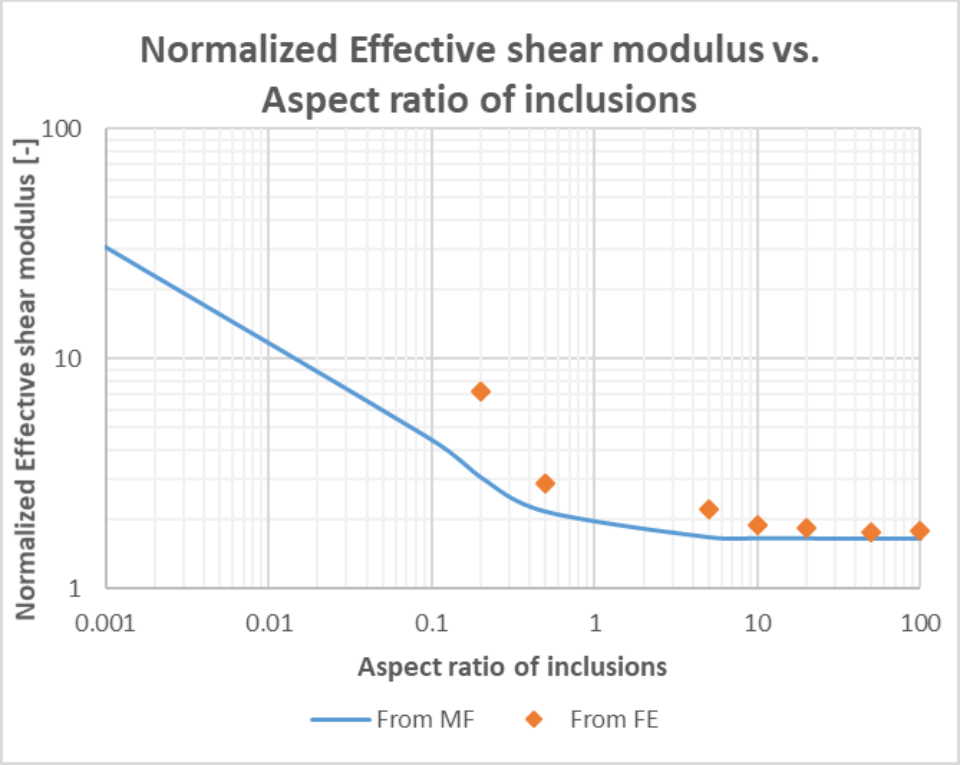

Figure 30 – $\bar{\mu}_{norm}$ vs aspect ratio of inclusions

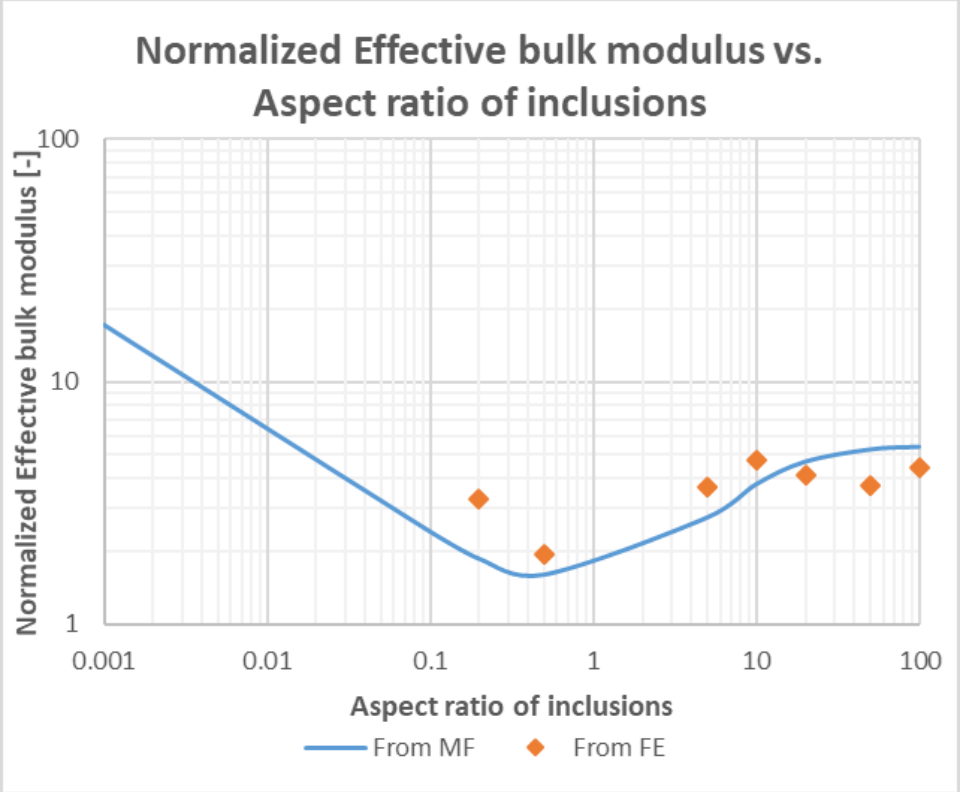

Figure 31 – $\bar{\kappa}_{norm}$ vs aspect ratio of inclusions

We observe that as the inclusions achieve the shape of fibers (high aspect ratio), the Digimat-FE results converge to the Digimat-MF results. This is because high aspect ratio involves uniform distribution of fibers in the RVE. Thus the microstructure becomes uniform, the resultant mesh quality is nicer and the results become more accurate. As we decrease the aspect ratio i.e. as the inclusions approach a platelet shape from the fiber shape, the error in the FE results increases with the highest error of 133% in $\bar{\mu}_{norm}$ and 75% in $\bar{\kappa}_{norm}$ for the aspect ratio 0.2.

For lower aspect ratios i.e. 0.1 and 0.001, when the inclusions are more like platelets, the mesh resulted in a huge number of mesh elements, which caused a spike in computational time. Varying the number of inclusions, the size of RVE, the reduction factor for inclusions and allowing the interpenetration of inclusions also did not result in an optimal mesh with good quality because of which, we were not able to get any results for both abovementioned aspect ratios.

4.4. Three-phase with Spherical Cavities and Prolate Reinforcements

The results obtained from Digimat-MF for the three phase microstructure with spherical cavities and prolate reinforcements calculated in subsection 3.3.2 are compared with the results obtained from Digimat-FE. The aspect ratio of the reinforcements is varied between 1 to 100.

The variations of $\bar{\mu}_{norm}$ and $\bar{\kappa}_{norm}$ with the aspect ratio of the reinforcements are shown in the plots below.

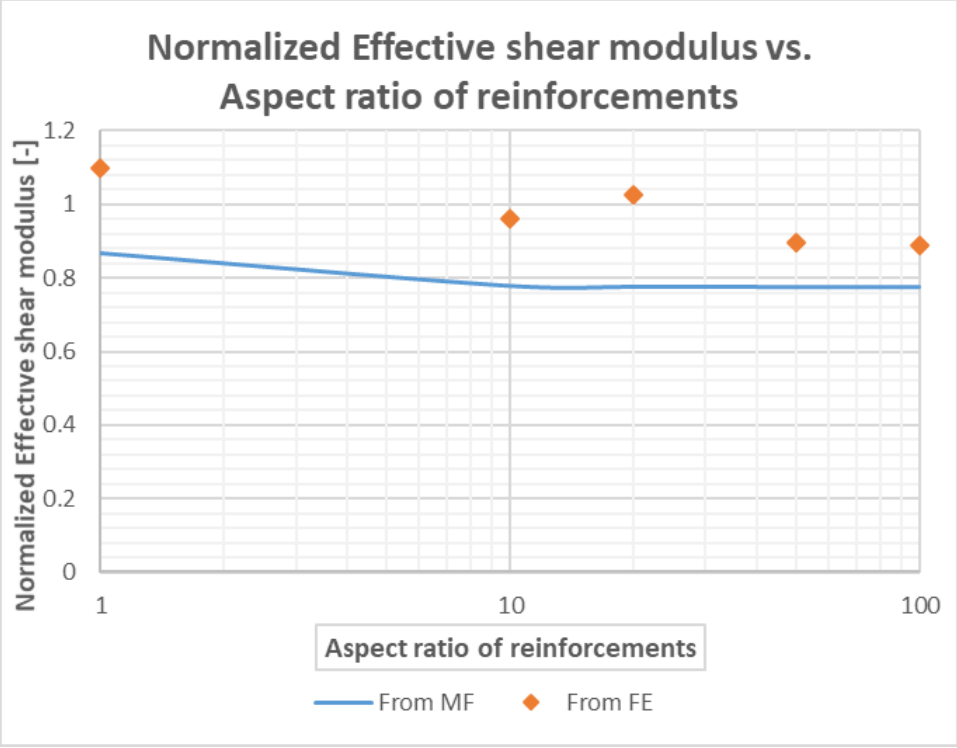

Figure 32 – $\bar{\mu}_{norm}$ vs aspect ratio of reinforcements

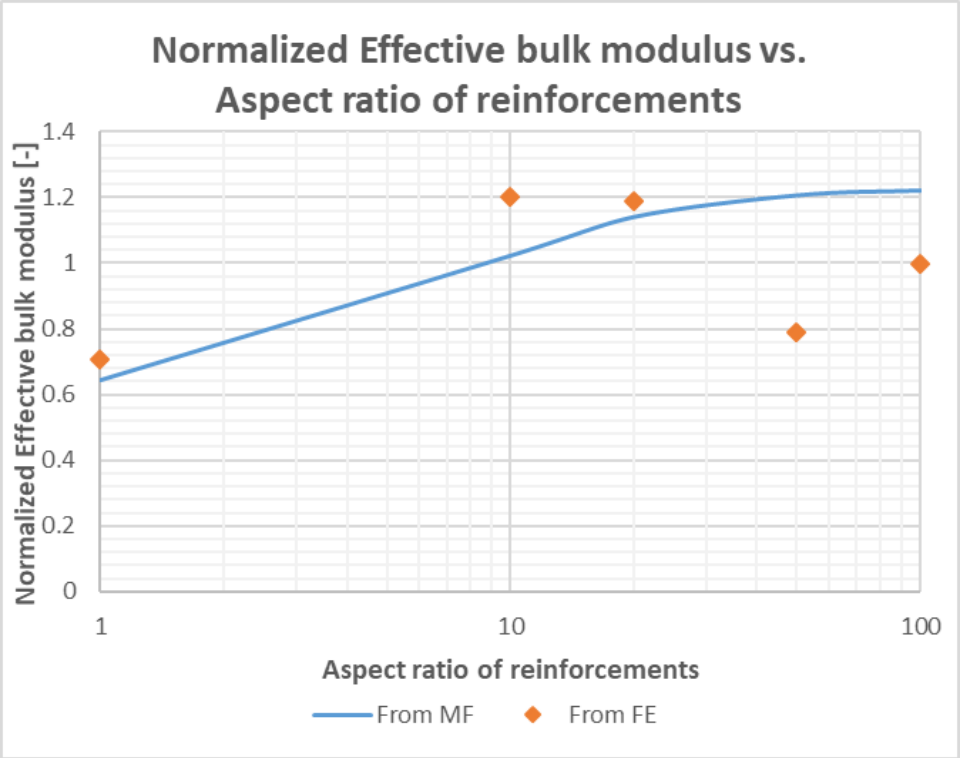

Figure 33 – $\bar{\kappa}_{norm}$ vs aspect ratio of reinforcements

Most of the FE results for $\bar{\mu}_{norm}$ and $\bar{\kappa}_{norm}$ correspond to the Digimat MF results. However, in some cases, the error becomes very high between results from the two methods. Due to the three phases in RVE, the optimal mesh quality is difficult to obtain. However, we can observe that the general trends of both FE and MF results are the same.

4.5. Three-phase with spherical reinforcements and oblate cavities

The results obtained from Digimat-MF for the three phase microstructure with spherical reinforcements and oblate cavities calculated in subsection 3.3.1 are compared with the results obtained from Digimat-FE. The aspect ratio of the reinforcements is varied between 0.001 to 100.

The variations of $\bar{\mu}_{norm}$ and $\bar{\kappa}_{norm}$ with the aspect ratio of the cavities are shown in the plots below.

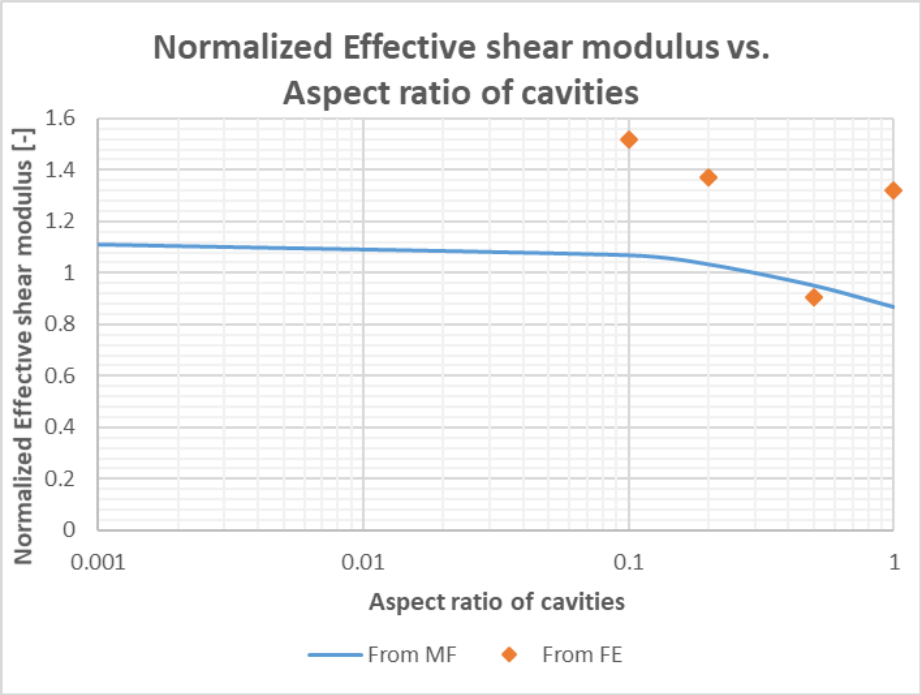

Figure 34 – $\bar{\mu}_{norm}$ vs aspect ratio of cavities

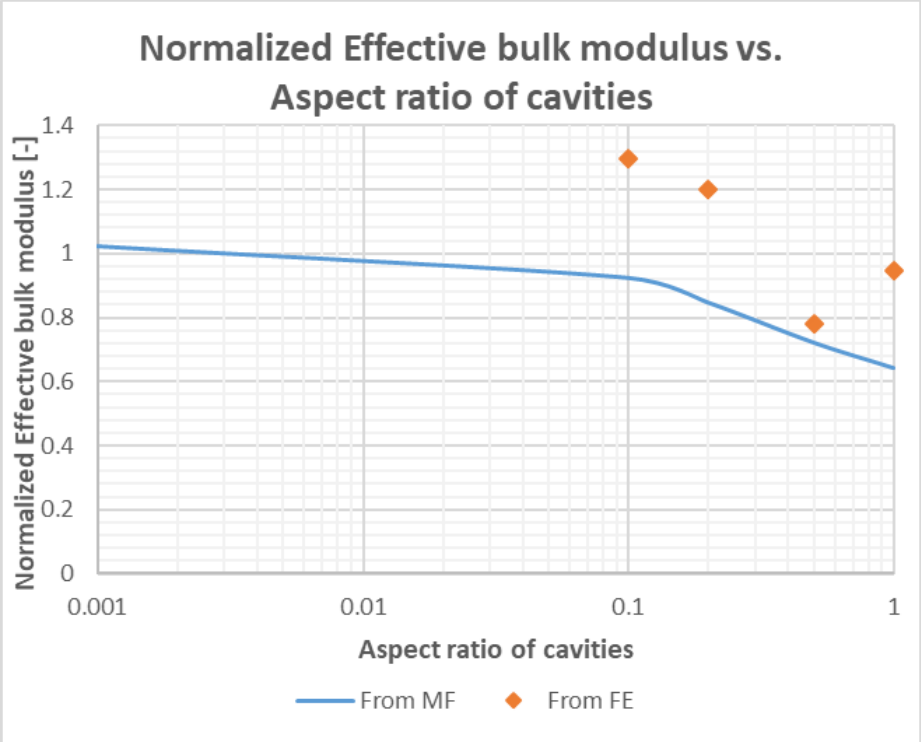

Figure 35 – $\bar{\kappa}_{norm}$ vs aspect ratio of cavities

Just like in the previous case, we observe some error in the $\bar{\mu}_{norm}$ and $\bar{\kappa}_{norm}$ results obtained from FE and MF. This is also because of the three phases in the RVE which results in difficulty to obtain an optimum mesh with appropriate volume fractions of the inclusions.

5. Conclusion:

In the two-phase materials case, the two mean-field models (Mori-Tanaka and Differential method) the predicted properties are closer to each other in smaller volume fractions. However, as we increase the volume fractions, they start to diverge after a value of volume fraction. Also, the predicted $\bar{\mu}$ and $\bar{\kappa}$ by Mori-Tanaka method are higher than the ones calculated using the differential method.

In the three-phase materials, the predicted properties computed using 4 different methods (2-step, 2-level-first and second variant, and differential model) are completely different from the other methods. In smaller volume fractions, $\bar{\mu}$ and $\bar{\kappa}$ are closer to each other in all 4 methods but as we increase the volume fractions, they deviate. In order to see which homogenization method predicts the better effective properties of the composite, experimental tests or high precision FE simulation should be performed and their results should be compared to the results obtained from each of these homogenization methods.

For a two-phase RVE, increasing the volume fraction of reinforcement results in the increase in $\bar{\mu}$ and $\bar{\kappa}$. Adding spherical cavities in a matrix results in lower $\bar{\mu}$ and $\bar{\kappa}$ of the RVE than that of the matrix. As the inclusions approach a fiber shape, the $\bar{\mu}$ and $\bar{\kappa}$ approach a constant value.

For a three-phase RVE, varying the aspect ratio of cavities from 0.001 to 0.1 with spherical reinforcements results in the significant decrease in the $\bar{\mu}$ and $\bar{\kappa}$. Whereas, in three-phase RVE with fiber-like reinforcements with spherical cavities, $\bar{\mu}$ and $\bar{\kappa}$ achieve a constant value.

Digimat-FE results for the three phase RVE contain a degree of error. This error increases as we decrease the aspect ratio of the inclusions or cavities. This error is because of the complicated mesh details and high number of mesh elements causing a significant increase in computational time. To save time, computational effort, and to ensure the reliability of results, other homogenization schemes should be used for the three-phase microstructures.